A Systems-Level ODE Model of B-Oxidation: Algorithmic Flux Optimization and Simulation of MCADD Pathophysiology

Ethan Shaw[1,2], Henry Chuo[2]

[1]Children's Nutrition Research Center, Department of Pediatrics, Baylor College of Medicine, Houston, TX, USA; [2]Department of Biomedical Engineering, University of Houston, Houston, TX, USA

July, 2025

Abstract

We introduce a computational model that simulates β-oxidation under varying metabolic conditions by solving a system of ordinary differential equations (ODEs) that describe the flux of key intermediates and cofactors. The model captures the stepwise breakdown of saturated, even-chain fatty acids, incorporating dynamic cofactor coupling and product drainage via infinite sinks to maintain numerical stability and biological realism. An optimization routine based on Nelder-Mead simplex refines initial conditions to minimize system residuals. When simulating medium-chain acyl-CoA dehydrogenase deficiency (MCADD), the model predicts metabolite accumulation upstream of the enzymatic block and downstream depletion – highlighting the sensitivity of flux distributions to enzymatic constraints. This work frames kinetic modeling as a tractable method to interrogate systems-level metabolic imbalance and offers a modular framework for future expansions.

Introduction

β-oxidation is a mitochondrial pathway that supports ATP synthesis via sequential cleavage of acyl-CoA substrates, particularly under fasting or exercise-induced states. The process begins with acyl-CoA activation in the cytoplasm, consuming ATP and producing AMP, before transport into the mitochondrial matrix through the carnitine shuttle. Inside the mitochondrion, β-oxidation proceeds through a cyclic sequence that generates acetyl-CoA, NADH, and $FADH_2$, which feed into the electron transport chain for further ATP synthesis [1].

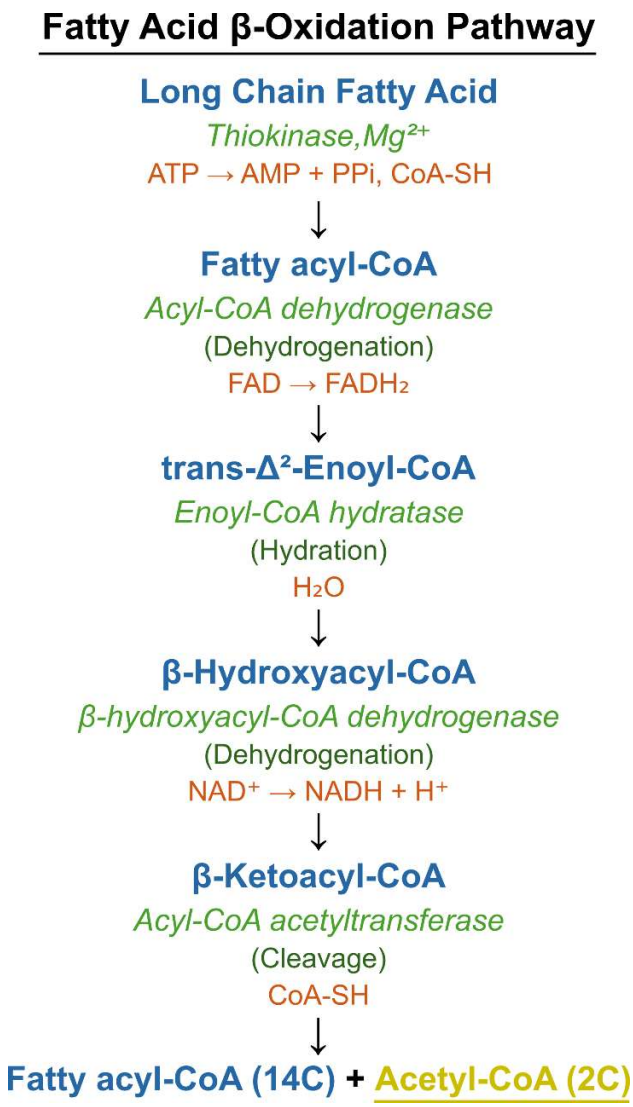

Figure 1. Pathway of Fatty acid Beta-Oxidation from long chain fatty acid to Fatty Acyl-CoA and Acetyl-CoA.

The biological significance of FAO lies in its role as a flexible energy source, especially under glucose-limiting conditions. Dysregulation of FAO – due to genetic mutations, enzyme deficiencies, or mitochondrial dysfunction – can lead to severe metabolic crises such as MCADD [4]. Quantitative modeling offers a means of simulating these perturbations by capturing transient imbalances and compensatory shifts in cofactor usage [2,5].

The goal of this study is to demonstrate how β-oxidation's fixed enzymatic steps and constrained stoichiometry can be modeled dynamically. Using ODE-based simulations, we interrogate both normal and pathological states, focusing on MCADD as a case study. While deliberately simplified to emphasize core pathway mechanics, this model establishes a foundation for modular extensions that can incorporate regulatory features in future work [6,7].

Methods

Model Construction

The β-oxidation pathway was modeled as a simplified kinetic scheme derived from five core enzymatic steps: thiokinase, first oxidation, hydration, second oxidation, and thiolysis. Reaction velocities were defined using mass-action kinetics, linearly proportional to substrate and cofactor concentrations [3]. Cofactors (ATP, FAD, NAD^+) were treated as variable, enabling dynamic depletion and regeneration. Downstream products were offloaded into infinite sinks (TCA cycle and ETC) for numerical stability [4].

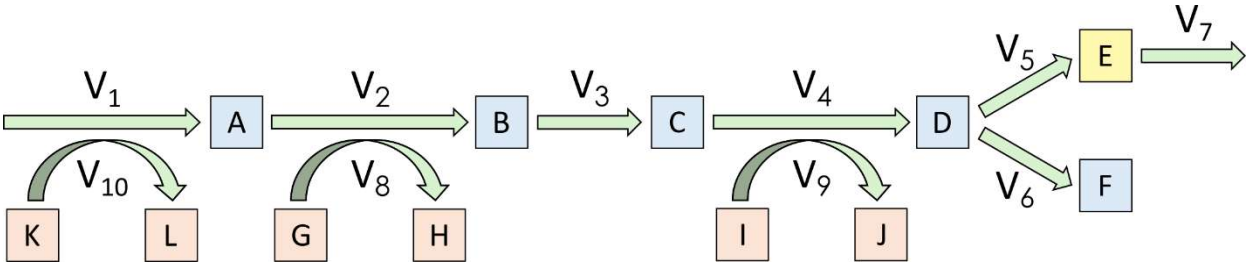

Figure 2. Beta-Oxidation pathway model from within the mitochondrial matrix. Used for equation derivation.

Reaction Components and Constants

A complete list of enzymes, cofactors, and metabolites is provided in Table 1. Reaction rate constants (k-values) were sourced from the BRENDA enzyme database [6] or inferred from comparable kinetic models [7,10], and are summarized in Table 2. Each enzymatic transformation was associated with an ODE, describing flux propagation across the system (Table 3).

Table 1. Components of Beta-Oxidation pathway model from within mitochondrial matrix.

Components of the β-Oxidation Model			
Type	Code	Name	Function
Enzyme	V1, V10	Thiokinase	Activates fatty acids for β-oxidation (requires ATP)
Enzyme	V2, V7, V8	Acyl CoA dehydrogenase	A → B (First oxidation)
Enzyme	V3	Enoyl CoA hydratase	B → C (Hydration)
Enzyme	V4, V9	β-Hydroxy acyl CoA dehydrogenase	C → D (Second oxidation)
Enzyme	V5, V6	Thiolase	D → E + F (Thiolytic cleavage)
Cofactor	G	FAD	Electron acceptor (first oxidation)
Cofactor	H	$FADH_2$	Reduced electron carrier (to ETC)
Cofactor	I	NAD^+	Electron acceptor (second oxidation)
Cofactor	J	NADH	Reduced electron carrier (to ETC)
Cofactor	K	ATP	Energy donor for fatty acid activation
Cofactor	L	AMP	Byproduct of ATP hydrolysis in activation step
Substrate	A	Fatty Acyl-CoA	Activated fatty acid
Substrate	B	Trans Δ2 Enoyl CoA	Intermediate (after first oxidation)
Substrate	C	β-Hydroxy acyl CoA	Intermediate (after hydration)
Substrate	D	β-Keto-acyl CoA	Intermediate (after second oxidation)
Substrate	F	Acyl-CoA	Shortened chain for next cycle (n-2 carbons)
Product	E	Acetyl-CoA	Product (enters citric acid cycle)

Table 2. Reaction rate constants (K-values) associated with key enzymes in the β-oxidation pathway, defining the kinetics of metabolic transformations.

Reaction Rate Constants		
Rate Constant	Value (1/s or 1/mM·s)	Reaction/Enzyme
k_1	0.05	Thiokinase (Acyl-CoA synthetase)
k_2	0.90	Acyl-CoA dehydrogenase reaction rate
k_3	1.20	Enoyl-CoA hydratase reaction rate
k_4	1.00	β-Hydroxy acyl-CoA dehydrogenase
k_5	1.10	Thiolase (Acyl-CoA Acetyltransferase)

Table 3. Reaction velocities and their corresponding ODEs in the β-oxidation model, describing the dynamic interactions governing metabolite flux.

Reaction Velocities and ODEs in Beta-Oxidation			
Reaction Velocity	Equation	Corresponding ODE	ODE Equation
V1	k1 * K	dA/dt	V1 - V2
V2	k2 * A * G	dB/dt	V2 - V3
V3	k3 * B	dC/dt	V3 - V4
V4	k4 * C * I	dD/dt	V4 - V6 - V5
V5	k5 * D	dE/dt	V5 - V7
V6	k5 * D	dF/dt	V6 - V10
V7	k2 * E	dG/dt	-V8
V8	k2 * A * G	dH/dt	V8
V9	k4 * C * I	dI/dt	V9
V10	k1 * K	dJ/dt	-V9
		dK/dt	-V10
		dL/dt	V10

Initial Conditions

Initial metabolite concentrations were selected from reported mitochondrial metabolomics data [8,9]. All concentrations were expressed in millimolar units to maintain dimensional consistency [7]. These values served as elastic parameters subject to optimization.

Table 4. Initial concentrations of metabolites used in the β-oxidation model, defining substrate availability and cofactor levels for testing.

Initial Concentrations of Metabolites in the Beta-Oxidation Model		
Variable	Initial Concentration (mM)	Description
A0	0.50	Fatty Acyl-CoA (depends on lipid metabolism rate)
B0	0.05	Trans Δ2 Enoyl-CoA (intermediate product)
C0	0.03	β-Hydroxy acyl-CoA (intermediate product)
D0	0.02	β-Keto acyl-CoA (intermediate product)
E0	1.50	Acetyl-CoA (enters citric acid cycle)
F0	0.20	Shortened Acyl-CoA (for next cycle)
G0	0.10	FAD (electron carrier)
H0	0.05	$FADH_2$ (reduced electron carrier)
I0	1.00	NAD^+ (electron acceptor for oxidation)
J0	0.50	NADH (reduced electron carrier)
K0	1.00	ATP (energy source for fatty acid activation)
L0	0.50	AMP (byproduct of ATP hydrolysis)

Computational Approach

Numerical integration was performed to simulate metabolite concentrations over time. MATLAB solvers (ODE45) were used with adaptive time-stepping [11]. To refine equilibrium conditions, initial concentrations were optimized using the Nelder-Mead simplex algorithm via FMINSEARCH, minimizing residual system concentration at t = 10 s [14].

Table 5. Algorithmic Workflow for β-Oxidation Simulation and Optimization.

Algorithm 1 ODE-Constrained β-Oxidation Simulation and Optimization

requirement 1: state order y = [A,B,C,D,E,F,G,H,I,J,K,L]
requirement 2: kinetics k = {k1=0.05, k2=0.9, k3=1.2, k4=1.0, k5=1.1} ◊ baseline rates
returns: trajectories y(t), terminal concentration Ctotal(T), summary tables/plots

```
function BOxSim(mode ∈ {baseline, optimized, MCADD})
  % INITIAL CONDITIONS (mM) → baseline block from code
  y0 ← [0.5, 0.05, 0.03, 0.02, 1.5, 0.2, 0.1, 0.05, 1.0, 0.5, 2.0, 0.1] ◊ stored 100 time points
  tspan1 ← linspace(0,10,100)                    ◊ fine grid for optimization runs
  tspan2 ← linspace(0,10,1000)
0.25
  define velocities (mass-action):
    V1=k1·K; V2=k2·A·G; V3=k3·B; V4=k4·C·I; V5=k5·D; V6=k5·D; V7=k2·E; V8=k2·A·G; V9=k4·C·I; V10=…

  define ODE f(y):
    dA= V1–V2;   dB= V2–V3;   dC= V3–V4;   dD= V4–V5–V6;
    dE= V5–V7;   dF= V6;      dG=–V8;      dH= V8;
    dI= V9;      dJ=–V9;      dK=–V10;     dL= V10;

  if mode = "baseline" then
    [t,y] ← ODE45(f, tspan1, y0)          ◊ adaptive RKF integration
    Ctotal(t) = ∑_i y_i(t)                ◊ diagnostic
    make_plots_and_tables(t,y,Ctotal)     ◊ total curve + per-metabolite figs
    return (t,y,Ctotal(10))
  end if

  if mode = "optimized" then
    J(y0^) := ∑_i y_i(T; ODE45(f,tspan2,y0^)) |        ◊ terminal |Ctotal|
    y0* ← fminsearch(J, [0.5,0.03,0.03,0.02,1.5,0.2,0.1,0.05,1.0,0.5,1.0,0.5])
    [t,y] ← ODE45(f, tspan2, y0*)
    Ctotal(t) = ∑_i y_i(t); emit_optimized_tables_and_plots(t,y,Ctotal)
    return (t,y,Ctotal(10))
  end if

  if mode = "MCADD" then
    fixedIdx ← [1,2,3,4,5]                ◊ disease routine with fixed indices
    y0_MC ← [5, 2.0, 0.01, 0.01, 0.01, 0.2, 0.1, 0.05, 1, 0.5, 1, 0.5]
    k2 ← ε (≪0)                           ◊ impair acyl-CoA dehydrogenase
    let optimIdx ← complement(fixedIdx)   ◊ variables allowed to change
    define J_MC(·):
      y0^ = y0_MC; y0^[optimIdx] = θ
      [t,y] ← ODE45(f, tspan1, y0^)
      return ∑_i y_i(T)
    θ* ← fminsearch(J_MC, y0_MC[optimIdx])   ◊ Nelder–Mead over free entries
    y0* ← y0_MC; y0*[optimIdx] = θ*
    [t,y] ← ODE45(f, tspan1, y0*)
    Ctotal(t) = ∑_i y_i(t); emit_MCADD_tables_and_plots(t,y,Ctotal)
    return (t,y,Ctotal(10))
  end if
end function
```

Results

Time-Course Simulation

Integration of the ODE system yielded directional mass flow through the β-oxidation pathway. While equilibrium was not achieved within the tested time window, metabolite concentrations exhibited expected trends of substrate depletion and product accumulation (Figure 3, Table 6) [10,11].

Table 6. Comparison of initial and final metabolite concentrations, illustrating substrate utilization and system balance at t = 10 (s)

Total Concentration of all Substrates at t = 10 (s)		
Metabolite	Starting Concentration (mM)	Final Concentration (mM)
Fatty Acyl-CoA	0.50	1.19E+00
Trans Δ2 Enoyl-CoA	0.05	1.60E-04
β-Hydroxy acyl-CoA	0.03	4.60E-04
β-Keto-acyl CoA	0.02	3.69E-04
Acetyl-CoA	1.50	1.51E-03
Acyl-CoA	0.20	2.99E-01
FAD	0.10	5.01E-05
FADH2	0.05	1.50E-01
NAD+	1.00	1.18E+00
NADH	0.50	3.21E-01
ATP	1.00	1.21E+00
AMP	0.50	8.87E-01
Final Concentration of Substrates (mM)		
5.239		

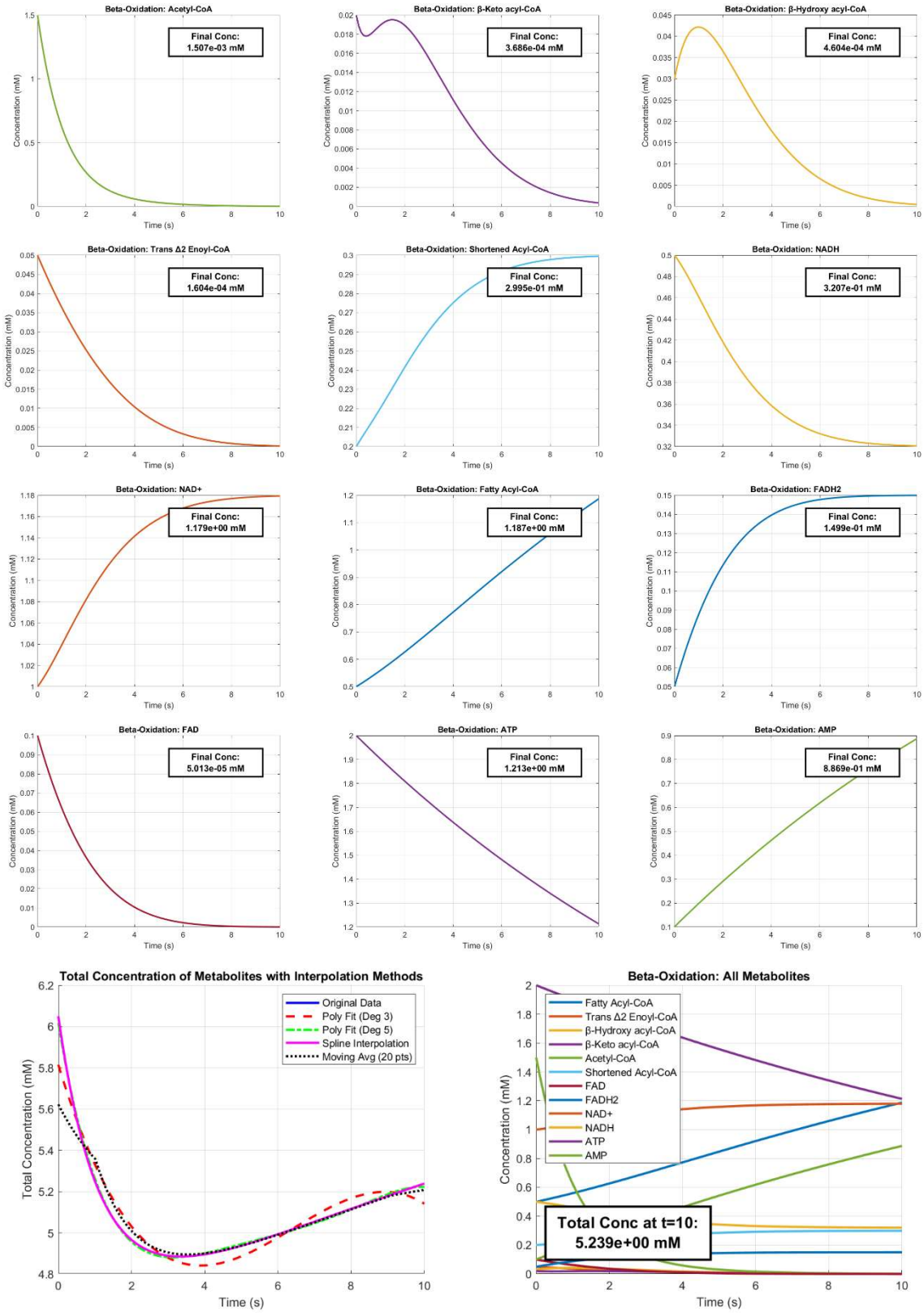

Figure 3. Time-series plots of individual metabolite concentrations and total system concentrations toward t = 10 (s).

Elastic Refinement

Without optimization, fixed enzyme kinetics and reaction structures prevented complete system balance. Optimization of initial conditions using Nelder-Mead simplex redistributed concentrations, enabling near-zero residual totals at t = 10 s (Table 7) [12,13].

Table 7. Comparison of initial, optimized, and final metabolite concentrations, showing how optimization balances fluxes to minimize total concentration at t =10

Comparison of Metabolite Concentrations: Initial, Optimized, and Final State			
Metabolite	Original Initial Concentration (mM)	Optimized Initial Concentration (mM)	Optimized Final Concentration (mM)
Fatty Acyl-CoA	0.50	5.97E-01	-2.39E-01
Trans Δ2 Enoyl-CoA	0.03	3.40E-02	-5.17E-03
β-Hydroxy acyl-CoA	0.03	4.19E-02	-3.93E-03
β-Keto-acyl CoA	0.02	1.48E-02	-1.22E-03
Acetyl-CoA	1.50	2.32E+00	2.57E-04
Acyl-CoA	0.20	4.86E-01	5.71E-01
FAD	0.10	1.09E-01	4.00E-02
FADH2	0.05	7.36E-02	1.43E-01
NAD+	1.00	7.86E-01	9.40E-01
NADH	0.50	2.69E-01	1.15E-01
ATP	1.00	-1.95E+00	-1.18E+00
AMP	0.50	3.91E-01	-3.76E-01
Final Concentration (mM) of Substrates (Initial Conditions) at t = 10 (s)			
5.239			
Final Concentration (mM) of Substrates (Optimized Conditions) t = 10 (s)			
-2.25119E-05			

MCADD Simulation

Pathological conditions were modeled by reducing k_2 (Acyl-CoA dehydrogenase) to near zero. This produced upstream accumulation of fatty acyl-CoA and trans Δ^2-enoyl-CoA, alongside depletion of downstream intermediates and acetyl-CoA. Flux bottlenecks mirrored clinically observed outcomes of impaired ketogenesis and hypoketotic hypoglycemia [4]. Optimized simulations restored partial system balance by adjusting metabolite pools (Tables 8–9, Figure 5) [2,5].

Table 8. Simulation parameters and resulting metabolic effects of Acyl-CoA dehydrogenase deficiency (MCADD), highlighting altered enzyme kinetics, substrate accumulation, intermediate buildup, and disrupted β-oxidation.

Simulating MCADD: Acyl-CoA Dehydrogenase Deficiency			
Parameter	Current Value	Modified Value (MCADD Simulation)	Effect
k_2 (Acyl-CoA Dehydrogenase)	0.9	0.01 – 0.00	Impaired enzyme function
A (Fatty Acyl-CoA)	0.50 mM	5.00 mM	Substrate accumulation
B (Trans Δ2 Enoyl-CoA)	0.05 mM	2.00 mM	Intermediate buildup
C0, D0, E0 (Downstream products)	Normal values	~0.01 mM	Lack of β-oxidation progression

Table 9. Simulation of MCADD disruptions due to reduced k_2, causing substrate accumulation, intermediate buildup, and impaired β-oxidation. Optimized metabolite concentrations illustrate adjustments restoring balance.

Optimized Metabolite Concentrations for Combating MCADD			
Metabolite	Original Initial Concentration (mM)	Optimized Initial Concentration (mM)	Optimized Final Concentration (mM)
Fatty Acyl-CoA	5.00	5.00E+00	2.20E+00
Trans Δ2 Enoyl-CoA	2.00	2.00E+00	1.42E-05
β-Hydroxy acyl-CoA	0.01	1.00E-02	1.03E-05
β-Keto-acyl CoA	0.01	1.00E-02	2.95E-05
Acetyl-CoA	0.01	1.00E-02	1.54E-03
Acyl-CoA	0.20	8.26E-01	1.95E+00
FAD	0.10	2.24E-01	1.86E-14
FADH2	0.05	1.41E-01	3.64E-01
NAD+	1.00	6.19E-01	2.85E+00
NADH	0.50	7.60E-01	-1.47E+00
ATP	1.00	-6.55E+00	-3.97E+00
AMP	0.50	6.62E-01	-1.92E+00
Final Concentration (mM) of Substrates (Optimized Conditions) at t = 10 (s)			
4.19309E-05			

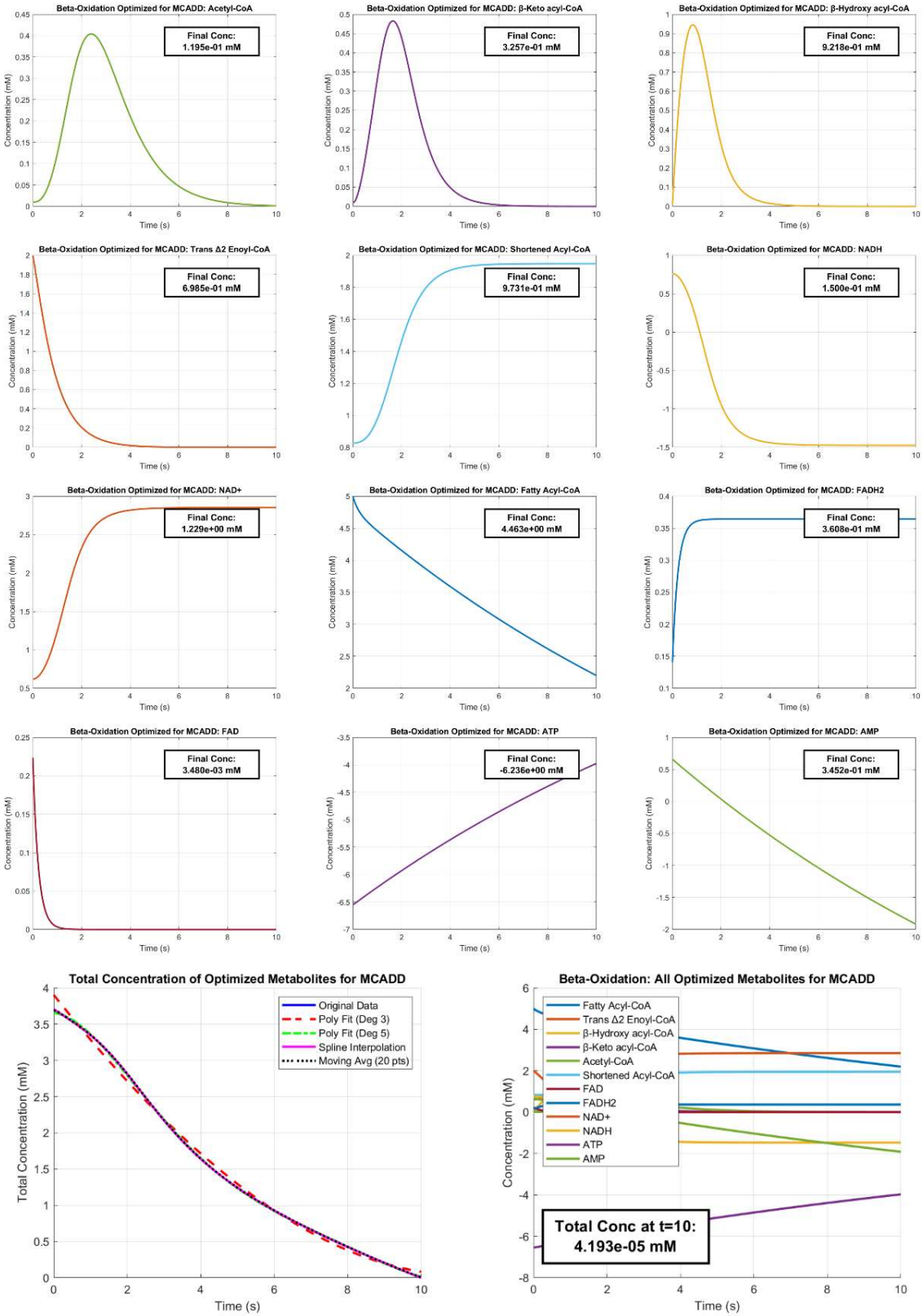

Figure 4. Time-series plots of individual metabolite concentrations and total system concentrations toward t = 10 (s) while optimized for Acyl-CoA Dehydrogenase Deficiency (MCADD) conditions.

Discussion

This study frames β-oxidation modeling as a tractable computational approach to metabolic disease analysis. By defining enzyme kinetics as inelastic variables and metabolite concentrations as elastic parameters, the model highlights the role of substrate availability in shaping system-level dynamics. Disease states such as MCADD emerge naturally from structural constraints in the ODE framework, producing physiologically consistent bottlenecks [12,13].

While simplifying assumptions (e.g., exclusion of the carnitine shuttle, feedback loops, or isoform-specific kinetics) limit scope, they also provide clarity and computational tractability [7]. The modular structure enables reintroduction of these elements in future iterations [16].

Importantly, the approach demonstrates how computational refinement of initial states can substitute for experimentally inaccessible adjustments in kinetic constants. This emphasizes the diagnostic potential of simulation frameworks for probing disease mechanisms and testing therapeutic strategies in silico [15,17].

Conclusion

We present an ODE-based kinetic model of β-oxidation that captures both physiological and pathological flux dynamics. Simulations highlight the sensitivity of metabolic pathways to enzymatic impairments, specifically MCADD, and demonstrate how elastic refinement can resolve imbalances. The framework offers a modular, reproducible foundation for future applications in metabolic diagnostics and therapeutic modeling [2,4,12].

Author Contributions

E.S. and H.C. conceived and developed the computational model. All MATLAB code, figures, and simulations were created independently by the authors. Both contributed equally to the manuscript.

Conflict of Interest

The authors declare no conflicts of interest.

Data and Code Availability

All source code and a step-by-step protocol are publicly available at: https://dx.doi.org/10.17504/protocols.io.x54v95yepl3e/v2

Cited Works

1. Karwi QG, Sun Q, Lopaschuk GD. *The Contribution of Cardiac Fatty Acid Oxidation to Diabetic Cardiomyopathy Severity*. Cells. 2021 Nov 21;10(11):3259. doi: 10.3390/cells10113259. PMID: 34831481; PMCID: PMC8621814. https://pmc.ncbi.nlm.nih.gov/articles/PMC8621814/

2. Modre-Osprian, Robert & Osprian, Ingrid & Tilg, Bernhard & Schreier, Günter & Weinberger, Klaus & Graber, Armin. (2009). Dynamic simulations on the mitochondrial fatty acid Beta-oxidation network. BMC systems biology. 3. 2. 10.1186/1752-0509-3-2.

3. Pedro Mendes, "The chemical logic behind Fatty Acid metabolism." University Fernando Pessoa, http://homepage.ufp.pt/pedros/bq/fatty.htm (accessed March 17, 2025).

4. Odendaal, C., Jager, E.A., Martines, AC.M.F. et al. Personalised modelling of clinical heterogeneity between medium-chain acyl-CoA dehydrogenase patients. BMC Biol 21, 184 (2023). https://doi.org/10.1186/s12915-023-01652-9

5. Abegaz F, Martines ACMF, Vieira-Lara MA, Rios-Morales M, Reijngoud DJ, et al. (2021) Bistability in fatty-acid oxidation resulting from substrate inhibition. PLOS Computational Biology 17(8): e1009259. https://doi.org/10.1371/journal.pcbi.1009259

6. Schomburg, I., Jeske, L., Ulbrich, M., et al. *BRENDA: The Comprehensive Enzyme Information System*. Leibniz Institute DSMZ – German Collection of Microorganisms and Cell Cultures. Available at: https://www.brenda-enzymes.org (accessed March 21, 2025).

7. Yasemi, M., & Jolicoeur, M. (2021). Modelling Cell Metabolism: A Review on Constraint-Based Steady-State and Kinetic Approaches. Processes, 9(2), 322. https://doi.org/10.3390/pr9020322

8. Ringel, A. E., Tucker, S. A., & Haigis, M. C. (2018). Chemical and Physiological Features of Mitochondrial Acylation. Molecular cell, 72(4), 610–624. https://doi.org/10.1016/j.molcel.2018.10.023

9. Carneiro, S., Pereira, R., & Rocha, I. (2014). Yeast metabolomics: sample preparation for a GC/MS-based analysis. Methods in molecular biology (Clifton, N.J.), 1152, 197–207. https://doi.org/10.1007/978-1-4939-0563-8_12

10. Kim, O. D., Rocha, M., & Maia, P. (2018). A Review of Dynamic Modeling Approaches and Their Application in Computational Strain Optimization for Metabolic Engineering. *Frontiers in microbiology*, *9*, 1690. https://doi.org/10.3389/fmicb.2018.01690

11. Postawa, K., Szczygieł, J., & Kułażyński, M. (2020). A comprehensive comparison of ODE solvers for biochemical problems. Renewable Energy, 156, 624-633.
12. Heinrich, R., & Rapoport, T. A. (1974). A linear steady-state treatment of enzymatic chains. General properties, control and effector strength. European journal of biochemistry, 42(1), 89–95. https://doi.org/10.1111/j.1432-1033.1974.tb03318.x
13. Kacser, H., & Burns, J. A. (1995). The control of flux. Biochemical Society transactions, 23(2), 341–366. https://doi.org/10.1042/bst0230341
14. Nelder, J. A., & Mead, R. (1965). A simplex method for function minimization. Computer Journal, 7(4), 308–313. https://doi.org/10.1093/comjnl/7.4.308
15. Bhatia, S. N., & Ingber, D. E. (2014). Microfluidic organs-on-chips. Nature Biotechnology, 32(8), 760–772. https://doi.org/10.1038/nbt.2989
16. Chen, J., Gomez, J. A., Höffner, K., Phalak, P., Barton, P. I., & Henson, M. A. (2016). Spatiotemporal modeling of microbial metabolism. BMC Systems Biology, 10, 21. https://doi.org/10.1186/s12918-016-0259-2
17. Libis, V., Delépine, B., & Faulon, J. L. (2016). Sensing new chemicals with bacterial transcription factors. Current Opinion in Microbiology, 33, 105–112. https://doi.org/10.1016/j.mib.2016.07.006

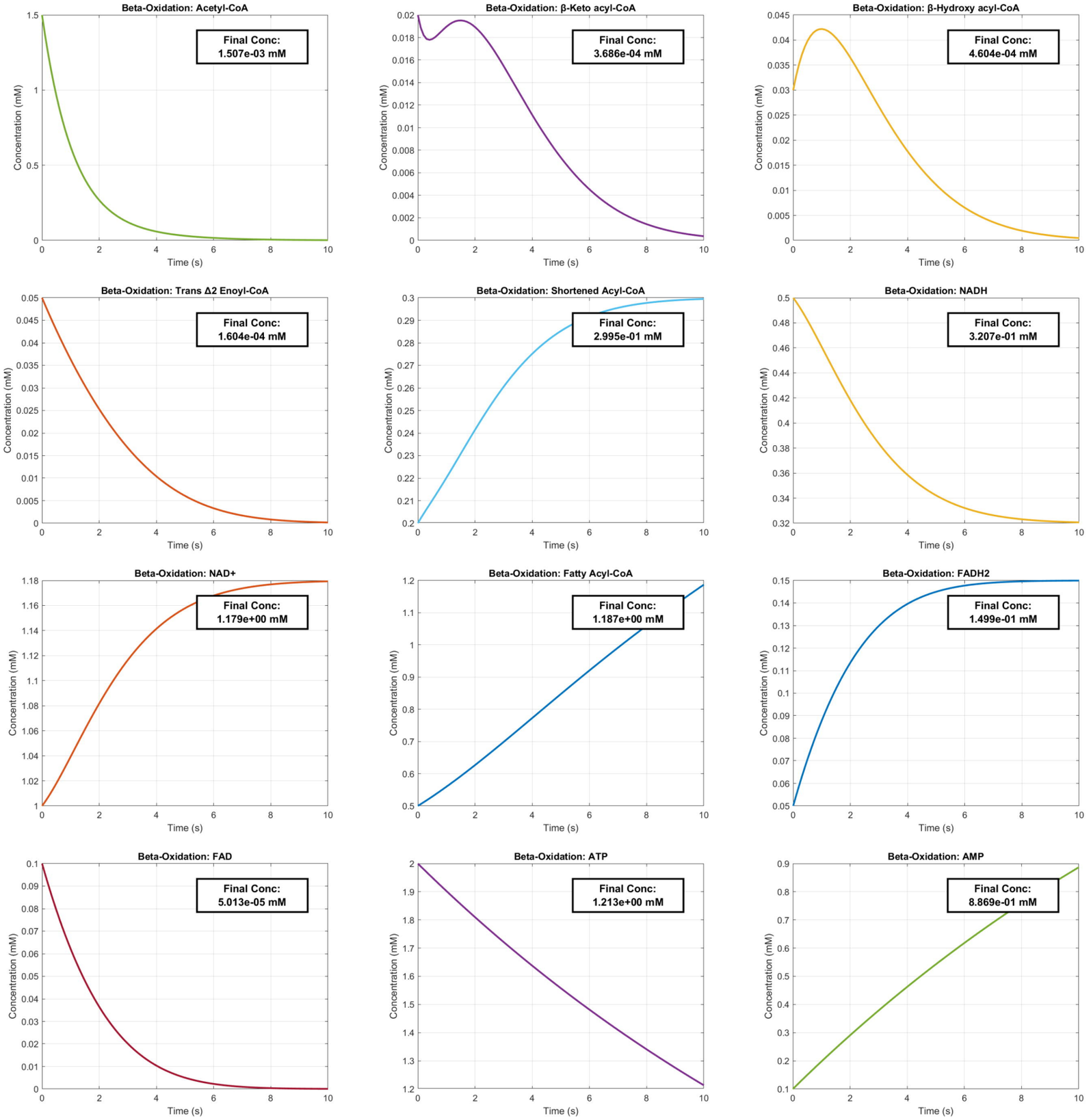
Beta-Oxidation: Acetyl-CoA
Final Conc: 1.507e-03 mM
Beta-Oxidation: β-Keto acyl-CoA
Final Conc: 3.686e-04 mM
Beta-Oxidation: β-Hydroxy acyl-CoA
Final Conc: 4.604e-04 mM
Beta-Oxidation: Trans Δ2 Enoyl-CoA
Final Conc: 1.604e-04 mM
Beta-Oxidation: Shortened Acyl-CoA
Final Conc: 2.995e-01 mM
Beta-Oxidation: NADH
Final Conc: 3.207e-01 mM
Beta-Oxidation: NAD+
Final Conc: 1.179e+00 mM
Beta-Oxidation: Fatty Acyl-CoA
Final Conc: 1.187e+00 mM
Beta-Oxidation: FADH2
Final Conc: 1.499e-01 mM
Beta-Oxidation: FAD
Final Conc: 5.013e-05 mM
Beta-Oxidation: ATP
Final Conc: 1.213e+00 mM
Beta-Oxidation: AMP
Final Conc: 8.869e-01 mM
Concentration (mM)
Time (s)

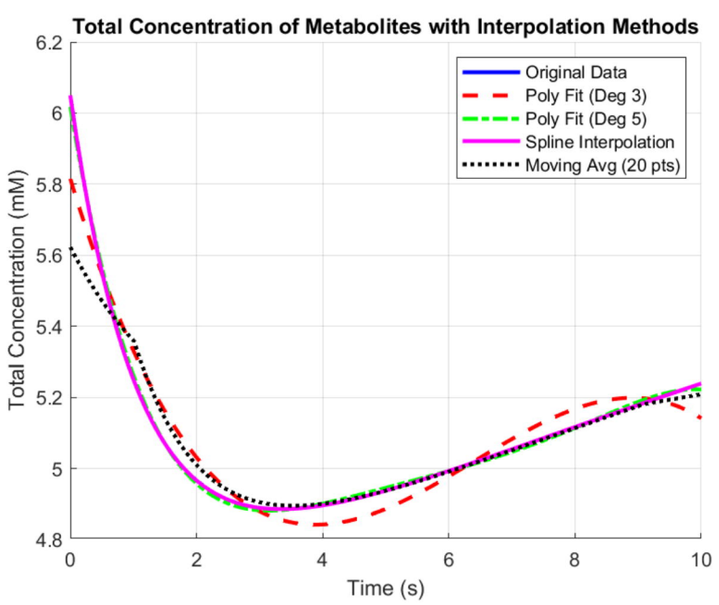
Total Concentration of Metabolites with Interpolation Methods
Original Data
Poly Fit (Deg 3)
Poly Fit (Deg 5)
Spline Interpolation
Moving Avg (20 pts)
Total Concentration (mM)
Time (s)

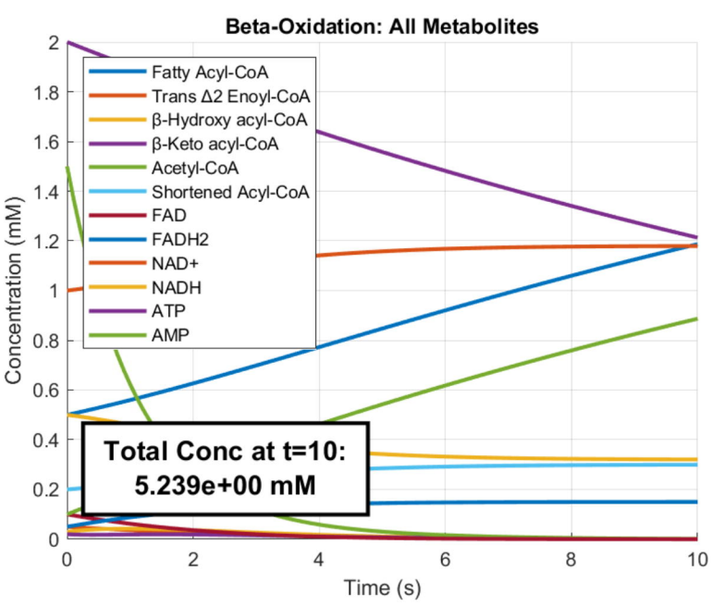
Beta-Oxidation: All Metabolites
Fatty Acyl-CoA
Trans Δ2 Enoyl-CoA
β-Hydroxy acyl-CoA
β-Keto acyl-CoA
Acetyl-CoA
Shortened Acyl-CoA
FAD
FADH2
NAD+
NADH
ATP
AMP
Total Conc at t=10:
5.239e+00 mM
Concentration (mM)
Time (s)

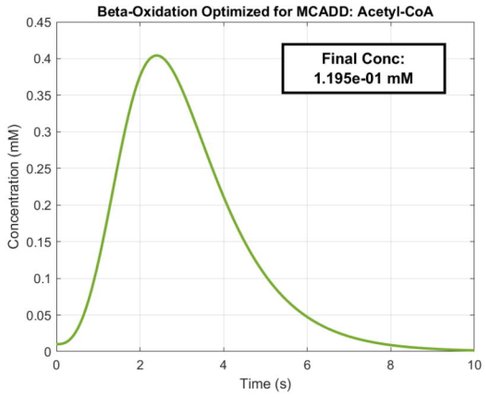
Beta-Oxidation Optimized for MCADD: Acetyl-CoA
Final Conc:
1.195e-01 mM
Concentration (mM)
Time (s)

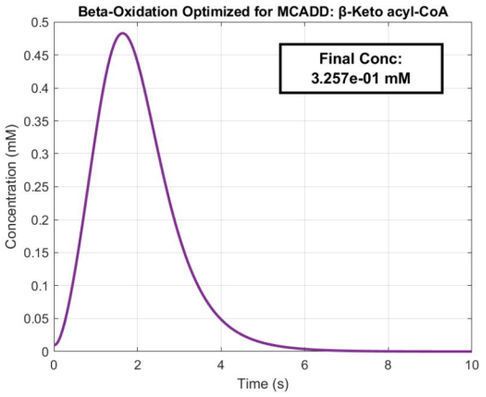
Beta-Oxidation Optimized for MCADD: β-Keto acyl-CoA
Final Conc:
3.257e-01 mM
Concentration (mM)
Time (s)

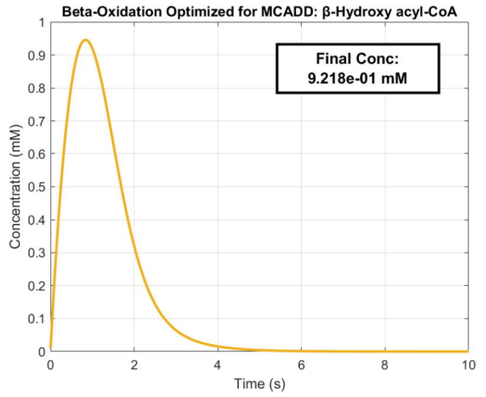
Beta-Oxidation Optimized for MCADD: β-Hydroxy acyl-CoA
Final Conc:
9.218e-01 mM
Concentration (mM)
Time (s)

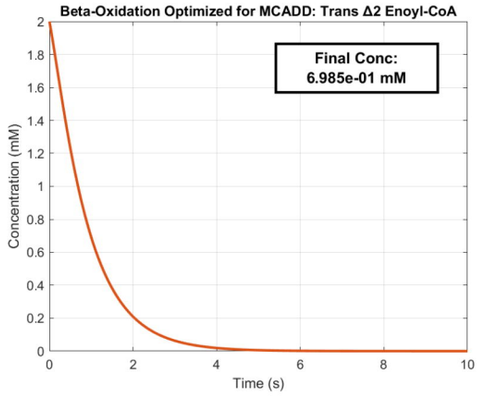
Beta-Oxidation Optimized for MCADD: Trans Δ2 Enoyl-CoA
Final Conc:
6.985e-01 mM
Concentration (mM)
Time (s)

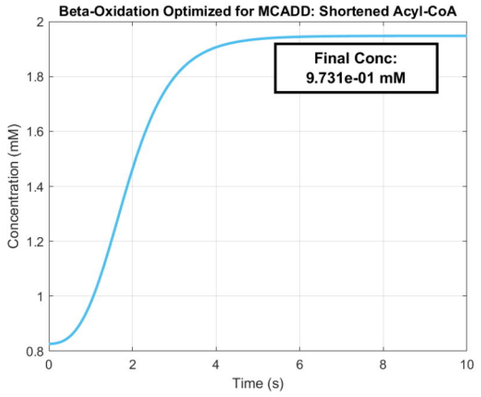
Beta-Oxidation Optimized for MCADD: Shortened Acyl-CoA
Final Conc:
9.731e-01 mM
Concentration (mM)
Time (s)

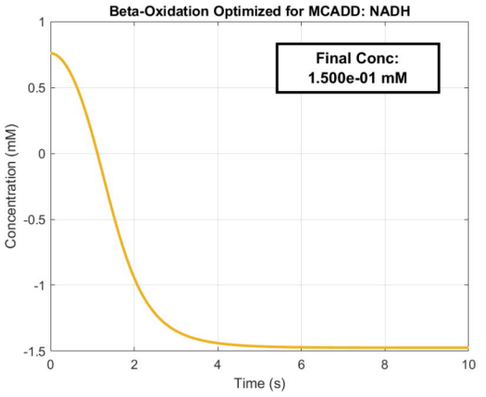
Beta-Oxidation Optimized for MCADD: NADH
Final Conc:
1.500e-01 mM
Concentration (mM)
Time (s)

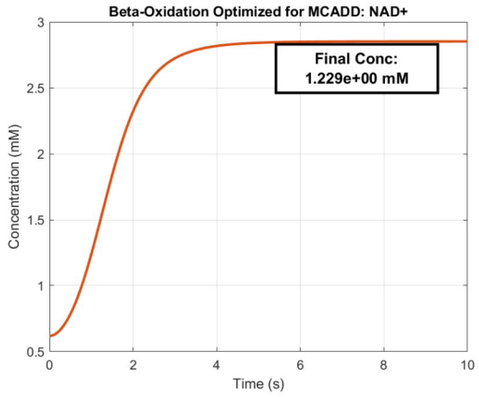
Beta-Oxidation Optimized for MCADD: NAD+
Final Conc:
1.229e+00 mM
Concentration (mM)
Time (s)

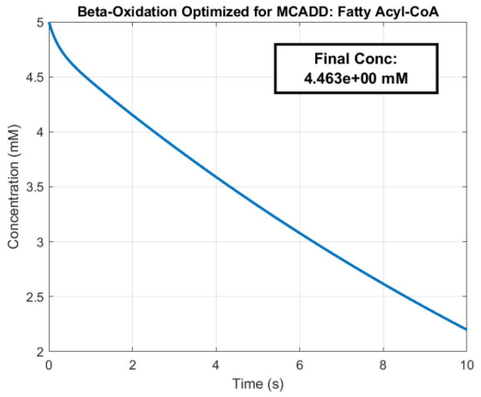
Beta-Oxidation Optimized for MCADD: Fatty Acyl-CoA
Final Conc:
4.463e+00 mM
Concentration (mM)
Time (s)

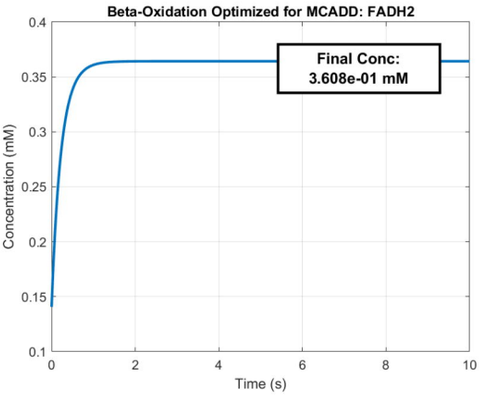
Beta-Oxidation Optimized for MCADD: FADH2
Final Conc:
3.608e-01 mM
Concentration (mM)
Time (s)

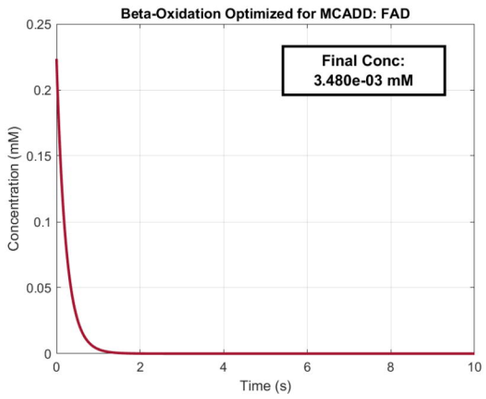
Beta-Oxidation Optimized for MCADD: FAD
Final Conc:
3.480e-03 mM
Concentration (mM)
Time (s)

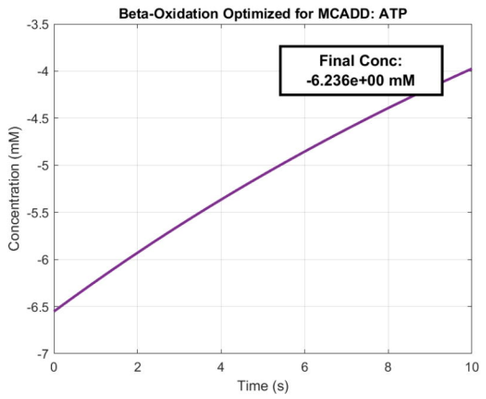
Beta-Oxidation Optimized for MCADD: ATP
Final Conc:
-6.236e+00 mM
Concentration (mM)
Time (s)

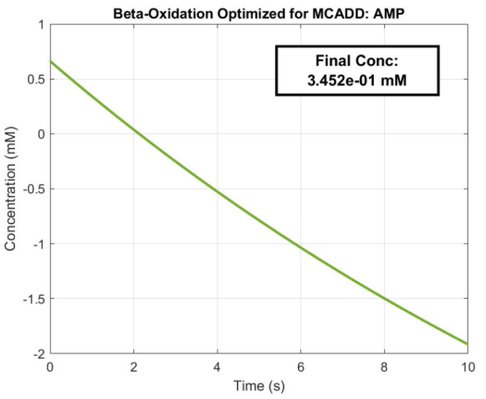
Beta-Oxidation Optimized for MCADD: AMP
Final Conc:
3.452e-01 mM
Concentration (mM)
Time (s)

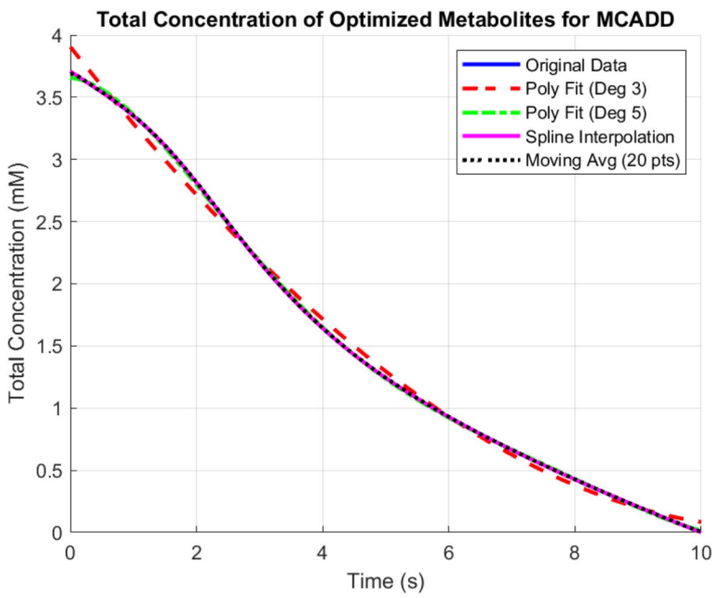
Total Concentration of Optimized Metabolites for MCADD
Original Data
Poly Fit (Deg 3)
Poly Fit (Deg 5)
Spline Interpolation
Moving Avg (20 pts)
Total Concentration (mM)
Time (s)

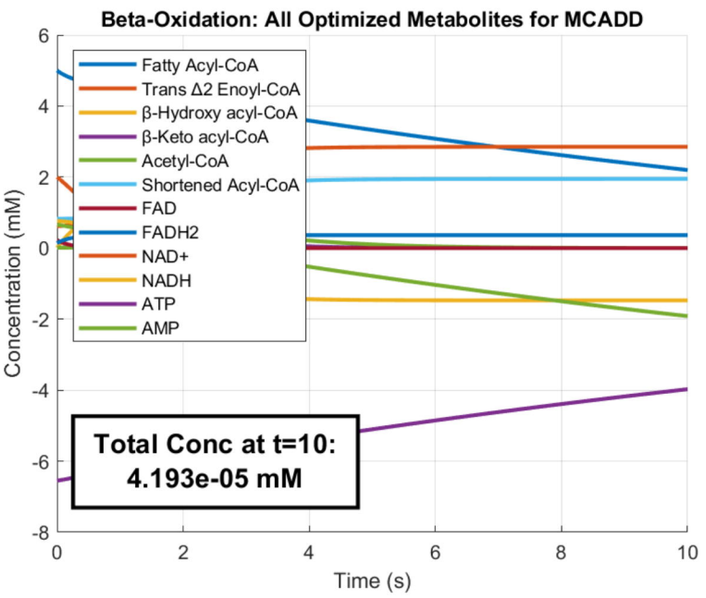
Beta-Oxidation: All Optimized Metabolites for MCADD
Fatty Acyl-CoA
Trans Δ2 Enoyl-CoA
β-Hydroxy acyl-CoA
β-Keto acyl-CoA
Acetyl-CoA
Shortened Acyl-CoA
FAD
FADH2
NAD+
NADH
ATP
AMP
Total Conc at t=10:
4.193e-05 mM
Concentration (mM)
Time (s)